Physics of the Earth and Planetary Interiors, 32 (1983) 193–202
Elsevier Science Publishers B.V., Amsterdam – Printed in The Netherlands

Solidus and liquidus temperatures and mineralogies for anhydrous garnet–lherzolite to 15 GPa

Claude T. Herzberg

Department of Geological Sciences, Rutgers University, New Brunswick, NJ 08903 (U.S.A.)

(Received November 18, 1982; accepted December 9, 1982)

Herzberg, C.T., 1983. Solidus and liquidus temperatures and mineralogies for anhydrous garnet–lherzolite to 15 GPa. Phys. Earth Planet. Inter., 32: 193–202.

A review of experimental data for systems pertaining to anhydrous fertile garnet–lherzolite shows strong convergence in the liquidus and solidus temperatures for the range 6.5–15 GPa. These can converge either to a common temperature or to temperatures which differ by only ~ 100°C. The major-element composition of magmas generated by even minor degrees of partial melting may be similar to the primordial bulk silicate Earth composition in an upper-mantle stratigraphic column extending over 160 km in depth.

The convergence of the solidus and liquidus temperatures is a consequence of the highly variable dT/dP of the fusion curves for minerals which crystallize in peridotite systems. In particular, dT/dP for the forsterite fusion curve is much less than that for diopside and garnet. Whether or not the solidus and liquidus intersect, the liquidus mineralogy for undepleted garnet–lherzolite compositions changes from olivine at low pressures to pyroxene, garnet, or a complex pyroxene–garnet solid solution at pressures in excess of 10–15 GPa. Geochemical data for the earliest Archean komatiites are consistent with an upper-mantle phase diagram having garnet as a liquidus phase for garnet–lherzolite compositions at high pressures. All estimates of the anhydrous solidus and liquidus for the range 10–15 GPa are consistent with silicate liquid compressibility data, which indicate that olivine may be neutrally buoyant in ultramafic magmas at these pressures.

1. Introduction

In order to gain a better understanding of crystallization and melting phenomena in the upper mantle, it is necessary that liquidus and solidus temperatures be characterized adequately. Progress in satisfying this basic requirement has been slow because of technical difficulties attending the generation of temperatures around 2000°C and pressures in excess of 5 GPa which are required in anhydrous melting experiments. Recently published experimental data on the fusion curve for forsterite to 15 GPa (Ohtani and Kumazawa, 1981) have provided the information necessary for more rigorously constraining anhydrous solidus and liquidus temperatures at all depths in the upper mantle. A review of these and other experimental data which bear on this problem is given here. The most important observation is that, contrary to existing petrological models, solidus–liquidus temperatures appear to converge to a common value in the 10–15 GPa pressure range for undepleted garnet–lherzolite compositions. There exists a wide pressure range in the upper mantle within which the major-element composition of magmas generated by even low degrees of partial melting may be similar to the primordial bulk silicate composition in this part of the Earth.

2. Experimental observations

Since olivine is likely to be the major liquidus phase for any bulk upper-mantle composition, such

0031-9201/83/$03.00

as that of garnet–lherzolite, the fusion curve for Mg_2SiO_4 (forsterite) provides an uppermost temperature bound. The curve shown in Fig. 1 summarizes the experimental data of Ohtani and Kumazawa (1981) to 15 GPa, and is in excellent agreement with earlier determinations by Davis and England (1964) to 4 GPa and Bowen and Andersen (1914) at 1 atm. Other components, such as Fe, Al, etc., will result in an olivine liquidus temperature which is lower than the forsterite fusion curve by a predictable amount which depends on the assumed mantle composition; the method for calculating these olivine liquidus temperatures has been given by Herzberg (1979).

A number of studies have chosen garnet–lherzolite PHN 1611 (37.33 wt. % MgO) as described by Nixon and Boyd (1973) as representative of undepleted mantle (Harrison, 1981; Mysen and Kushiro, 1977). At 1 atm. olivine is on the liquidus at 1700 ± 30°C, a temperature which is insensitive to variations in $K_{D,ol-l}^{Fe-Mg}$. For average garnet–lherzolite as given by Carswell (1968; 41.00% MgO), the liquidus temperature is 1725 ± 30°C at 1 atm. Much higher temperatures can arise only from more refractory compositions; for a 100% dunite rock of Fo_{93} (i.e., 52% MgO), the liquidus is at 1850°C. For any given bulk composition the liquidus temperature at 1 atm. can be extrapolated parallel to the forsterite fusion curve, because variations in K_D with pressure are small (Longhi et al., 1978). The average upper-mantle liquidus shown in Fig. 1 is for a range of undepleted garnet–lherzolite compositions identified above with 37–41% MgO.

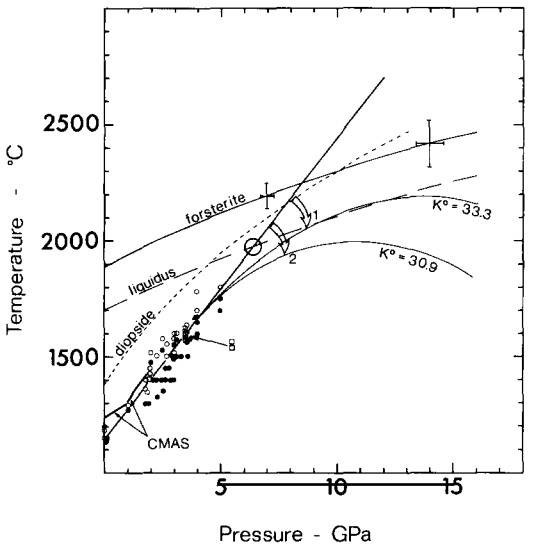

Fig. 1. Experimental constraints on the anhydrous upper-mantle solidus and liquidus. Closed circles, all solid; open circles, crystals + liquid, for natural complex systems referenced in text. The curve labeled CMAS is the solidus for the system $CaO–MgO–Al_2O_3–SiO_4$ (Presnall et al., 1979). Squares are the solidus determined for a fertile garnet–peridotite composition, PHN 1611 (Mysen and Kushiro, 1977; Harrison, 1981). The open triangle is the estimated solidus for the system diopside–pyrope–forsterite (Davis and Schairer, 1965). The curve labeled forsterite is its fusion curve, with error bars (Ohtani and Kumazawa, 1981). The dotted curve is the diopside fusion curve determined experimentally to 5 GPa and extrapolated to higher pressures using the Simon equation given in the text. The large circle positions the solidus–liquidus intersection according to a linear extrapolation of the solidus. The curves marked 1 and 2 are two alternatives to the linear solidus. The values of $K°$ for magmas along each solidus are in units of GPa and for $K' = 5$.

Experimental data used to bracket the solidus in simple and complex lherzolite compositions are also shown in Fig. 1. Despite the wide range of compositions used in the nine independent experimental determinations (Davis and Schairer, 1965; Ito and Kennedy, 1967; Kushiro et al., 1968; Green and Ringwood, 1970; Howells et al., 1975; Mysen and Kushiro, 1977; Presnall et al., 1979; Harrison, 1981; the data of Arndt (1976) for a komatiite composition are included), the interlaboratory agreement is excellent, enabling a solidus with a linear dT/dP of 130°C/GPa to be defined rigorously to 5 GPa. This agreement is surprising, because the solidus for natural complex systems is in fact a divariant transition zone of ~ 60°C within which liquid, olivine, two pyroxenes, and one phase of plagioclase, spinel or garnet can coexist (Mysen and Kushiro, 1977; Fujii and Scarfe, 1983); that is, it is more difficult to define than the solidus for CMAS (Fig. 1), which is strictly univariant.

It should be noted that although the data can be fitted to a linear solidus, the detailed work of Presnall et al. (1979) for CMAS shows a curvature with dT/dP decreasing with increasing pressure. This is consistent with all fusion curves, and it will be argued that it applies equally to the mantle solidus for complex systems at pressures higher than 5 GPa.

3. Analysis of experimental observations

It can be seen from Fig. 1 that a linear extrapolation of the solidus results in convergence of the solidus and liquidus temperatures at a common value of ~ 1970°C at 6.5 GPa. The question of whether in fact convergence occurs at this low pressure, at higher pressures, or at all is addressed below. If indeed it does occur, it can be understood in part by considering the phase relations for the system Mg_2SiO_4–$CaMgSi_2O_6$ shown in Fig. 2. The T–X locations of the pseudobinary eutectic at 1 atm. and at 1 and 2 GPa have been determined experimentally by a number of investigators, and the results summarized by Presnall et al. (1978). The most fundamental observation is that the composition of the first partial melt of the bulk compositions B located at X shifts to more olivine-rich composition with increasing pressure, a concept which is central to models of basalt petrogenesis advanced by O'Hara (1968) and subsequent adherents. The eutectic compositions and temperatures at pressures greater than 2 GPa are illustrative approximations only, estimated using the fusion curves for forsterite and diopside as a guide; these are shown in Fig. 1. The melting curve for diopside to 5 GPa has been determined experimentally (Williams and Kennedy, 1969) and is here extrapolated to higher pressures by means of the Simon equation $P = 37.07\ [(T/1665)^3 - 1]$. As long as the heats of fusion of forsterite and diopside change by similar amounts along their fusion curves and there are no major changes in the activity–composition relations for the liquid components in the melt phase, dT/dX for the diopside and forsterite crystallization fields should be approximately the same at low and high pressures (i.e., in fact, dT/dX for each will probably increase if ΔH_{fusion} is lowered along the fusion curve, resulting in a sharper "V" in the eutectic valley). Because the fusion curve for diopside has a much larger dT/dP than that for forsterite, as seen in Fig. 1, the diopside field expands faster than that for forsterite for any given increment of pressure. The intersection of the two defines the eutectic X, which thus shifts to more forsterite-rich compositions with increasing pressure. As long as the fusion curves for the minerals involved in melting phenomena have positive dT/dP and X shifts toward the bulk composition B with increasing pressure, a reduction in the solidus–liquidus temperature interval for B will be inevitable. In the example in Fig. 2, ΔT for the solidus and liquidus is reduced from 430°C at 1 atm., to 60°C at 7.5 GPa, and to 0°C at 10 GPa, where the bulk composition B melts directly to a liquid of its own composition. At higher pressures, a model peridotite composition B must have diopside as its liquidus phase. At even higher pressures, a singular point is established at which pure forsterite (or its spinel polymorph) begins to melt incongruently to diopside + liquid.

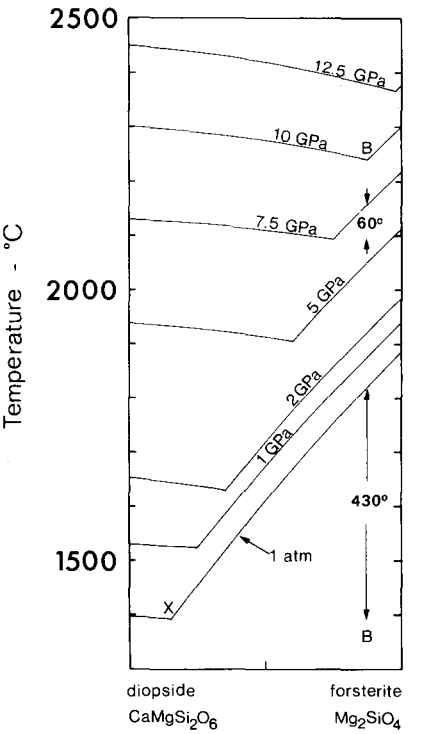

Fig. 2. Approximate locations of the pseudobinary eutectic for the join diopside–forsterite to high pressures. The locations of each end-member are given in Fig. 1. As long as the first partial melt at X shifts to the bulk composition B with increasing pressure, the solidus–liquidus temperature interval for B must diminish. At ~ 10 GPa the solidus and liquidus converge to a common temperature, and a model peridotite composition B can melt directly to a liquid of its own composition. At higher pressures the first partial melt approaches the composition of forsterite, and the liquidus phase for B can be diopside.

Although the illustration in Fig. 2 involves only two mineral phases and is rather simple, the experimental data in Fig. 1 suggest that convergence might also hold for natural complex compositions. This would appear to indicate that the simple binary model in Fig. 2 may not break down seriously when the primary phase volumes of garnet and enstatite are also considered for natural complex systems. This is unusual, because the possibility that the primary phase volumes of olivine, low-Ca pyroxene, high-Ca pyroxene, and garnet would intersect exactly at the bulk mantle composition (i.e., and worse still, at a range of possible bulk compositions) at some T and P appears rather remote. However, it is necessary to consider the validity of four primary phase volumes existing at 2200°C and 10–15 GPa. For example, the low- and high-Ca pyroxene primary phase volumes, which are separated by a cotectic equilibrium at low pressures, may be transformed into a single primary phase volume with a broad thermal minimum if complete solid solution exists between the two end-members for the conditions of interest (e.g., Herzberg, 1978). This would be analogous to the quartz and alkali feldspar primary phase volumes for the ternary system SiO_2–$NaAlSi_3O_8$–$KAlSi_3O_8$ at 1 atm. (Tuttle and Bowen, 1958). Additionally, experimental results for the join $Mg_4Si_4O_{12}$–$Mg_3Al_2Si_3O_{12}$ and for PHN 1611 show that up to 30 mol % of the garnet phase has the composition of pyroxene at 1000–1200°C and 14.6 GPa (Akaogi and Akimoto, 1979). At solidus temperatures a significant amount of garnet can also be dissolved into pyroxene (e.g., Herzberg, 1978). The possibility that there exists a complete solid solution between garnet and pyroxene along the solidus must be seriously entertained. Since the fusion curve for pyrope garnet to 10 GPa has a slope about equal to that for diopside (Ohtani et al., 1981), the primary phase field for garnet may expand as rapidly as that for diopside in Fig. 2 for any given increment of pressure. The phase relations for garnet–lherzolite in a compositional space defined by a tetrahedron with olivine, diopside, enstatite and garnet at the corners could thus be described in terms of two primary phase volumes, these being olivine and a complex pyroxene–garnet solid solution. The first partial melt of a range of possible garnet–lherzolite compositions could be defined by a thermal minimum with a wide compositional trough, much like petrogeny's residua system for SiO_2–$NaAlSi_3O_8$–$KAlSi_3O_8$ at 1 atm. The simple model in Fig. 2 could then be modified to a cross-section in the above tetrahedral composition space, with the diopside liquidus replaced by a complex pyroxene–garnet solid solution. The wide compositional trough would have to be characterized by expanding the binary system in Fig. 2 to a ternary system. Although an undepleted garnet–lherzolite may not melt *directly* to a liquid of its own composition, only a very small temperature increase of 1–10°C above the solidus may be needed for complete melting to occur. If three primary phase volumes exist, these being for olivine, a pyroxene phase, and garnet, it is unlikely that the solidus and liquidus will intersect; however, they may approach each other to within 10–100°C. Whatever the correct interpretation may be, the experimental data in Fig. 1 demonstrate clearly that the solidus–liquidus temperature interval must become very small at high pressures; although the detailed phase relations remain obscure, the first partial melt compositions at very high pressures must be more similar to those for a range of possible mantle lherzolite compositions than at pressures closer to the surface of the Earth. These phase relations are very similar to those for the system $NaAlSiO_4$–SiO_2 explored by Bell and Roseboom (1969), and are discussed in more detail below.

Another problem is whether this apparent solidus–liquidus temperature intersection occurs along the 130°C/GPa linear solidus extrapolation located at ~ 1970°C and 6.5 GPa, or at some higher pressure along a curved solidus. If indeed the former is correct, there would have to be a major discontinuous change in the subsolidus mineralogy at this pressure, resulting in a strong discontinuous decrease in dT/dP for the solidus at higher pressures. Since no phase change is known to occur at these conditions for an olivine-dominated mineralogy, this alternative must be abandoned in favor of a strongly curved solidus. If the only criterion for estimating the extrapolated solidus location is that it be always less than liquidus temperatures, the two solidi shown in

Fig. 1 are probable choices. Although it remains to be established rigorously, it is difficult to avoid a geometry such that at some point dT/dP becomes zero. This can happen in the 11–14 GPa range, and thereafter the slope can be negative. Either the solidus and liquidus converge to a common T and P, as indicated by Model 1, or the solidus is so strongly curved, as in Model 2, that no intersection with the liquidus is possible.

A thermodynamic analysis would now be of value in order to assess the validity of the two possible solidus curves in the 10–15 GPa range of geological interest. The analysis which follows proceeds, however, with the inadequate assumption that the solidus curvature can be understood by analogy with the thermodynamic behavior of a simple mineral fusion curve. This assumption is inadequate because, unlike a simple fusion curve, the subsolidus mineralogy does not usually melt to a liquid of its own composition, and the composition of the melt phase at the solidus varies considerably with pressure (e.g., Fig. 2). In the analysis which follows, an approximate estimate is made of the compressibility of magmas along the solidus, and this information is compared with existing data.

The slope of any fusion curve at any T and P is determined by the Clausius–Clapeyron relation

$$dT/dP = \Delta V/\Delta S \qquad (1)$$

which becomes progressively reduced with pressure in large part because of a continuous reduction in the ΔV term (but see also the discussion below). For any solid (s) or liquid phase (l), it is possible to write

$$V/V^0 = \rho^0/\rho$$
$$= \left[1 + \alpha(T - T_r)\right]\left(PK'/K^0 + 1\right)^{-1/K'} \qquad (2)$$

where ρ and V are the density and volume at the T and P of interest, ρ^0 and V^0 are the density and volume at 1 atm. and the reference temperature T_r, α is the thermal expansivity (i.e., $1/V(\partial V/\partial T)_P$), and K^0 and K' are the isothermal bulk modulus and its pressure derivative, respectively.

It can be seen that the strength of the curvature of a melting relation will depend strongly on changes in the ΔV term; in particular, where $dT/dP = 0$, $\Delta V = 0$ and $V_s = V_l$ for simple mineral fusion curves. Because silicate liquids are usually less dense than silicate solids at any T and P, it is clear that $\Delta V = 0$ only if the liquid phase is considerably more compressible than the solid phase. Indeed, in a review of the existing data, Stolper et al. (1981) have presented evidence suggesting that silicate liquids may be about an order of magnitude more compressible than silicate solids, with basaltic magmas having $K_l^0 = 11.5$–20.0 GPa at $K' = 6$–7. These estimates may be compared with those derived from Figs. 1 and 3 and eqs. 1 and 2 for densities of magma compositions ranging from garnet–lherzolite PHN 1611 to tholeiite. These calculations are based on the assumption that the densities of magmas and olivine are the same or very similar when dT/dP for the solidus $\rightarrow 0$. As long as this assumption is not seriously in error, the compressibilities of complex magma compositions calculated using eqs. 1 and 2 for simple fusion curves should be reasonable approxima-

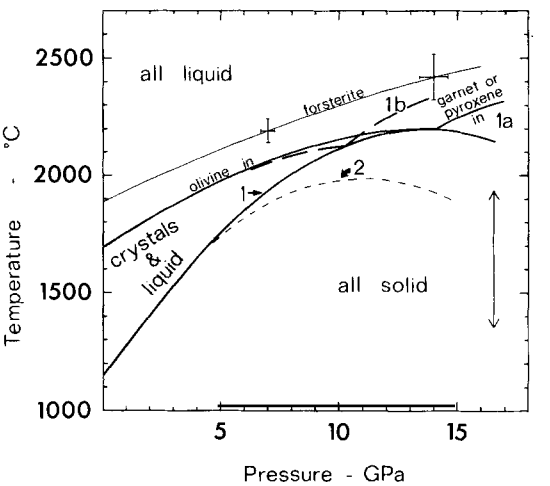

Fig. 3. Several possible solidus–liquidus topologies for fertile garnet–lherzolite to 15 GPa. In Model 1 (heavy lines) the solidus and liquidus converge to a common value; 1a and 1b are two possible intersection locations. In Model 2 (light broken lines) the solidus and liquidus converge but do not intersect. The liquidus temperatures and mineralogies for Model 2 should be similar to those for Model 1 indicated by "olivine in" and "garnet or pyroxene in". The vertical arrow brackets the range of present-day geotherm locations as cited in the text for ~15 GPa. The real solidus location is probably located somewhere between 1 and 2.

tions. The strength of the solidus curvature will also be due to an increase in the olivine normative content of magmas with increasing pressure. In simple systems, such as in Fig. 2, dT/dP for both the solidus and the liquidus are obviously identical at a forsterite singular point at pressures greater than ~ 12.5 GPa.

A strongly curved solidus which converges with the liquidus may have a number of topologies similar to the possible cases shown in Fig. 3. In the case of Model 1a, dT/dP for both the solidus and liquidus $\rightarrow 0$ at the T and P of convergence. In Model 1b, these slopes can remain small but positive where they converge, the solidus dT/dP becoming zero at some higher pressure. Model 1b can be representative of the situation in which $\Delta\rho$ (olivine–magma) $\neq 0$ where $dT/dP = 0$, or $\Delta\rho = 0$ where $dT/dP \neq 0$. In Models 1a and 1b the liquidus mineralogy changes from olivine to another at pressures greater than the convergence point, possibly becoming pyroxene, garnet, or a complex pyroxene–garnet solid solution.

Although dT/dP for the liquidus is considered to be zero at the point of convergence in Model 1a, the slope as deduced from the forsterite fusion curve appears to remain positive, as shown in Fig. 1. However, the error bars are totally consistent with the possibility that $dT/dP = 0$ at high pressures, indicating that pure forsterite may be neutrally buoyant with a liquid of its own composition at ~ 15 GPa. Of greater relevance would be well-established solidus and liquidus curves for a composition containing some Fe. Although pure forsterite may remain more dense than a liquid of its own composition, in complex systems the preferential partitioning of the heavy element Fe in the liquid phase may be instrumental in promoting a density inversion. Indeed, it has been demonstrated by experiment and calculation that this partitioning results in the flotation of olivine on top of its coexisting Fe-enriched liquids for intermediate compositions on the join Mg_2SiO_4–Fe_2SiO_4 at 1 atm. (Herzberg et al., 1982).

The density of olivine of Fo_{93} is compared initially to the density of primitive garnet–lherzolite liquid PHN 1611 for Models 1a and 2. For Model 1a, dT/dP for both the liquidus and the solidus $\rightarrow 0$ at their point of intersection at 2200°C and 14 GPa. For Model 2, dT/dP for the solidus $\rightarrow 0$ at 2000°C and 11 GPa. An olivine of composition Fo_{93} is particularly suitable, because the density of its liquid counterpart is almost identical to the density of PHN 1611 liquid at 1 atm. The liquidus temperature T_r at 1 atm. is 1700°C, and the parameters may be assigned as follows: $\rho_s^0 = 3.11$ g cm^{-3} (Fisher and Medaris, 1969; Hazen, 1976), ρ_l^0 (PHN 1611 liquid) $= 2.74$ g cm^{-3} (Nelson and Carmichael, 1979), $\alpha_s = 3.8 \times 10^{-5}$ °C^{-1} (Hazen, 1976), $\alpha_l = 7.1 \times 10^{-5}$ °C^{-1} (Nelson and Carmichael, 1979), $K_s^0 = 128$ GPa and $K_s' = 5$ (Kumazawa and Anderson, 1969), and $K_l' = 5$ (Stevenson, 1980; Stolper et al. (1981) used values of 6–7). It is assumed that the densities of olivine and ultramafic liquid are the same where $dT/dP \rightarrow 0$ along the solidi, these being 3.30–3.33 g cm^{-3} between 11 and 14 GPa in the range 2000–2200°C. Stolper et al. (1981) and Nisbet and Walker (1982) have suggested that this olivine–magma density inversion may occur at pressures as low as 4–9 GPa, on the basis of compressibility information for simple binary melt compositions and some natural basaltic compositions. Solving now for K_l^0 results in values of 30.9–33.3 GPa, as shown in Fig. 1; these become 24.2–25.2 GPa if $K_l' = 7$ instead of 5. Although these are somewhat higher than the values suggested by Stolper et al. (1981), in general the agreement is very good.

The calculation above is now repeated but with a new set of parameters which are representative of magmas having low olivine normative contents at low pressures. The density of Fo_{93} is compared with the density of a liquid with the composition of average FAMOUS glass, having $\rho_l^0 = 2.70$ g cm^{-3} at $T_r = 1150$°C (Elthon, 1979; Nelson and Carmichael, 1979; T_r is now the 1 atm. solidus in Fig. 1). This is conceptually equivalent to considering the density of olivine in relation to the eutectic X in Fig. 2 at 1 atm., instead of composition B at 10 GPa as was done above. For solidi 1 and 2, K_l^0 ranges from 20.9 to 22.8 GPa for $K' = 5$, and 15.1 to 16.0 GPa for $K' = 7$. These are in excellent agreement with the values summarized by Stolper et al. (1981). They are also in excellent agreement with those estimated independently for tholeiitic to komatiitic liquids, calculated from partial molar and volume fraction compressibili-

ties of oxide components in silicate liquids; these in turn were estimated from a thermodynamic analysis of fusion curves for simple minerals (Herzberg, in preparation).

The absolute T–P location and topology of the solidus and liquidus curves in the 10–15 GPa range as suggested in Fig. 3 will certainly be subject to change upon calibration by experiment. However, it is emphasized that they are constrained by the raw experimental data for the forsterite fusion curve, and the solidus is constrained to lie within 300°C from 5 GPa to the pressure at which a liquidus phase other than olivine becomes stable; clearly, the existence of components other than those in forsterite will reduce this 300°C interval by a significant amount, the best estimates of which are given in Figs. 1 and 3. Moreover, these phase equilibria are totally consistent with current estimates of the isothermal bulk modulus for silicate liquids, although the values of K_1^0 so calculated above are obviously not the products of a rigorous thermodynamic analysis. The important suggestion that olivine may have neutral buoyancy in magmas at high pressures (Stolper et al., 1981) is now supported by a number of independent observations. However, if the assumption in the above analysis is correct, namely that $\Delta\rho \rightarrow 0$ where dT/dP for the solidus $\rightarrow 0$, the pressure at which this density crossover takes place is in the range 11–14 GPa, rather than 4–9 GPa as favored by Stolper et al. (1981) and Nisbet and Walker (1982). The higher pressure estimate for complex systems is favored but not required by dT/dP for the fusion curve for forsterite, which remains positive to zero over the pressure range of 1 atm. to 15 GPa. The higher pressure for the density crossover arises mainly from the choice of parameters used in an equation of state and the calculation of liquid densities along a solidus rather than isothermally; this requires the inclusion of a thermal expansivity term in the equation of state.

4. Some phase relations for the upper mantle and some geological consequences

In the absence of experimental data for the range 10–15 GPa, it is not possible to determine which of the topologies in Fig. 3 is most appropriate for an undepleted garnet–lherzolite composition such as PHN 1611. However, there are a number of geological consequences which are common to all topologies, and there are others which are unique to each. Models 1a and 1b suggest that there exists a finite depth at which a fertile garnet–lherzolite composition can melt to a liquid of its own composition within a temperature interval of 1–10°C. Model 2, however, indicates that the first partial melt composition may *approach* the bulk upper-mantle composition, but can never be identical to it.

If indeed Models 1a and 1b are most appropriate, the temperature interval between the solidus and liquidus may be less than ~ 100°C over an extended pressure interval of ~ 8 to 13 or 15 GPa. This is equivalent to a stratigraphic section of more than 160 km in the lower reaches of the upper mantle. In both Models 1 and 2, the first partial melt composition may be very similar to that of the bulk silicate Earth at a range of depths; however, if Model 1 should be shown to be preferable to Model 2, such primordial magma compositions would extend over a much deeper section of the upper-mantle column. Similarly, if Model 1 is favored, the first partial melt composition may be very similar in its major-element geochemistry to a magma produced by 100% melting, and this may take place over a temperature interval which is only tens of degrees above the solidus at pressures far removed from the convergence point. Since the density contrast between olivine and ultramafic magmas (and pyroxenes?) would also be minimal at these pressures, fractional crystallization and melting processes similar to those which operate near the Earth's surface would not operate as efficiently to modify the partial melt products of any primordial silicate Earth at high pressures. Only by such mechanisms as garnet fractionation and flow differentiation during convection could phase separation have occurred during dry melting episodes. It is within this stratigraphic section of the upper mantle that the most primordial silicate Earth compositions should be located, if, indeed, they exist at all.

The phase relations shown in Models 1a and 1b are very similar to those for the simpler system

$NaAlSiO_4$–SiO_2 explored by Bell and Roseboom (1969) and discussed by Presnall et al. (1979). For bulk compositions between albite and jadeite, the solidus and liquidus converge to a common value between the jadeite and albite singular points located at 2.7 and 3.2 GPa, respectively. In this system, dT/dP for the solidus becomes negative at pressures higher than that which defines the albite singular point, because the assemblage jadeite + liquid is denser than albite. The equivalent in Fig. 3 would be the emergence of an olivine singular point (or transition zone) where $dT/dP = 0$ in Model 1b, at 2200°C and 14 GPa. Here a forsteritic olivine could melt directly to a liquid of its own composition, and at yet higher pressures it could melt incongruently to another phase (i.e., pyroxene–garnet solid solution?) + liquid. As for the system $NaAlSiO_4$–SiO_2, the actual T–P location at which the solidus and liquidus converge (e.g., Models 1a and 1b) would be dependent on the bulk composition. For more tholeiitic or eclogitic compositions (e.g., more diopside-rich than *B* in Fig. 2), the intersection may be at substantially lower pressures than those for Model 1b in Fig. 3.

If Model 2 is the most appropriate characterization of the phase relations, the solidus may converge to within 10–100°C of the liquidus in the range 10–15 GPa. Although the first partial melt composition cannot be the same as an undepleted garnet–lherzolite mantle at any pressure, the two can be very similar. The extent to which they differ can then be measured indirectly by the solidus–liquidus temperature contrast.

Figure 3 shows that the liquidus mineralogy in Model 2 may also change from olivine at low pressures to pyroxene, garnet, or a complex pyroxene–garnet solid solution in the range 10–15 GPa. If this should occur, olivine might then be the second phase to appear in the isobaric crystallization of a garnet–lherzolite magma at high pressures. If the solidus remains at much lower temperatures than the liquidus, owing to the development of a strongly negative dT/dP, as indicated in Fig. 3, the anhydrous melting temperatures near the base of the upper mantle would have to be lower than all previous estimates. In particular, the high melting temperatures for the upper part of the lower mantle suggested by Watt and Ahrens (1982; 2500–3500°C) could be seriously in error. In order to evaluate these possibilities more fully, the solidus in Models 1 and 2 will have to be extended to pressures at which a modified spinel polymorph of $(Mg, Fe)_2SiO_4$ and eventually (Mg, Fe)O + $(Mg, Fe)SiO_3$ (pv) or 2(Mg, Fe)O + SiO_2 (st) are the stable subsolidus phases. However, a cursory inspection of the solidus locations in relation to various estimates of the present-day geotherm (Stacey, 1977; Brown and Shankland, 1981; Richter and McKenzie, 1981; Anderson, 1982) in Fig. 3 suggests that widespread melting would have to be anticipated in the range 16.5–20 GPa if indeed solidus 2 with a strongly negative slope is valid. Since no low-velocity zone occurs at these pressures *at the present time*, the actual solidus will probably be located somewhere between Models 1 and 2 in Fig. 3.

Common to both Models 1 and 2 is the probability that the liquidus mineralogy for a garnet–lherzolite composition will change from olivine at low pressures to pyroxene, garnet, or a complex pyroxene–garnet solid-solution phase in the range 10–15 GPa. This is totally consistent with the geochemical identity of early Archean komatiites from the Overwacht group, Amitsoq enclaves and India, as summarized by Jahn et al. (1982). These older komatiites appear to have substantially higher CaO/Al_2O_3 and Gd/Yb ratios than later Archean komatiites, which show variable but near-chondritic ratios. Fractionation of garnet has been suggested (Jahn et al., 1982) and is fully compatible with either Model 1 or 2 at pressures at which a post-olivine liquidus phase becomes stable. Later Archean komatiites showing near-chondritic Gd/Yb and variable CaO/Al_2O_3 ratios near the chondritic value could be explained by modest olivine and pyroxene fractionation at lower pressures. Although only one post-olivine liquidus phase is shown in Fig. 3, the sequence may be something like olivine–pyroxene–garnet–perovskite or olivine–pyroxene + garnet solid solution–perovskite from 1 atm. to pressures in excess of 15 GPa. One obvious consequence of this is that any secular variation in the geochemical identity of komatiites may be a record of this liquidus sequence, reflecting crystallization histories which evolved to or recorded only progressively shallower depths in the mantle with time.

Acknowledgements

This research was supported by NASA under Grant NAGW-177. Comments by Dave Walker improved an early draft of this paper.

References

Akaogi, M. and Akimoto, S., 1979. High-pressure phase equilibria in a garnet lherzolite, with special reference to Mg^{2+}–Fe^{2+} partitioning among constituent minerals. Phys. Earth Planet. Inter., 19: 31–51.

Anderson, O.L., 1982. Are anharmonicity corrections needed for temperature-profile calculations of interiors of terrestrial planets? Phys. Earth Planet. Inter., 29: 91–104.

Arndt, N.T., 1976. Melting relations of ultramafic lavas (komatiites) at 1 atm. and high pressure. Carnegie Inst. (Washington) Yearbook, 75: 555–562.

Bell, P.M. and Roseboom Jr., E.H., 1969. Melting relationships of jadeite and albite to 45 kilobars with comments on melting diagrams of binary systems at high pressures. Mineral. Soc. Am., Spec. Pap., 2: 151–162.

Bowen, N.L. and Andersen, O., 1914. The binary system MgO–SiO_2. Am. J. Sci., 4th Ser., 37: 487–500.

Brown, J.M. and Shankland, T.J., 1981. Thermodynamic parameters in the Earth as determined from seismic profiles. Geophys. J., 66: 579–596.

Carswell, D.A., 1968. Possible primary upper mantle peridotite in Norwegian basalt gneiss. Lithos, 1: 322–355.

Davis, B.T.C. and England, J.L., 1964. The melting of forsterite up to 50 kbar. J. Geophys. Res., 69: 1113–1116.

Davis, B.T.C. and Schairer, J.F., 1965. Melting relations in the join diopside–forsterite–pyrope at 40 kilobars and at one atmosphere. Carnegie Inst. (Washington) Yearbook, 64: 123–126.

Elthon, D., 1979. High magnesia liquids as the parental magma for ocean floor basalts. Nature, 278: 514–518.

Fisher, G.W. and Medaris Jr., L.G., 1969. Cell dimensions and X-ray determinative curve for synthetic Mg–Fe olivines. Am. Mineral., 54: 741–753.

Fujii and Scarfe, 1983. Equilibration experiments between peridotites and basalts: 1 Composition of liquids co-existing with spinel lherzolite at 10 kbar and the genesis of MORB. Contrib. Mineral. Petrol., in press.

Green, D.H. and Ringwood, A.E., 1970. Mineralogy of peridotitic compositions under upper mantle conditions. Phys. Earth Planet. Inter., 3: 359–371.

Harrison, W.J., 1981. Partitioning of REE between minerals and coexisting melts during partial melting of a garnet–lherzolite. Am. Mineral., 66: 242–259.

Hazen, R.M., 1976. Effect of temperature and pressure on the crystal structure of forsterite. Am. Mineral., 61: 1280–1293.

Herzberg, C.T., 1978. Pyroxene geothermometry and geobarometry: experimental and thermodynamic evaluation of some subsolidus phase relations involving pyroxenes in the system CaO–MgO–Al_2O_3–SiO_2. Geochim. Cosmochim. Acta, 42: 945–957.

Herzberg, C.T., 1979. The solubility of olivine in basaltic liquids: an ionic model. Geochim. Cosmochim. Acta, 43: 1241–1251.

Herzberg, C.T., Baker, M.B. and Wendlandt, R.F., 1982. Olivine flotation and settling experiments on the join Mg_2SiO_4–Fe_2SiO_4. Contrib. Mineral. Petrol., 80: 319–323.

Howells, S., Begg, C. and O'Hara, M.J., 1975. Crystallization of some natural eclogites and garnetiferous ultrabasic rocks at high pressure and temperature. Phys. Chem. Earth, 9: 895–902.

Ito, K. and Kennedy, G.C., 1967. Melting and phase relations in a natural peridotite to 40 kilobars. Am. J. Sci., 265: 519–538.

Jahn, B.-M., Gruau, G. and Glikson, A.Y., 1982. Komatiites of the Onverwacht Group, S. Africa: REE geochemistry, Sm/Nd age and mantle evolution. Contrib. Mineral. Petrol., 80: 25–40.

Kumazawa, M. and Anderson, O.L., 1969. Elastic moduli, pressure derivatives and temperature derivatives of single crystal olivine and single crystal forsterite. J. Geophys. Res., 74: 5961–5972.

Kushiro, I., Syono, Y. and Akimoto, S.-I., 1968. Melting of a peridotite nodule at high pressures and high water pressures. J. Geophys. Res., 73: 6023–6029.

Longhi, J., Walker, D. and Hays, J.F., 1978. The distribution of Fe and Mg between olivine and lunar basaltic liquids. Geochim. Cosmochim. Acta, 42: 1545–1558.

Mysen, B.O. and Kushiro, I., 1977. Compositional variations of coexisting phases with degrees of melting of peridotite in the upper mantle. Am. Mineral., 62: 843–865.

Nelson, S.A. and Carmichael, I.S.E., 1979. Partial molar volumes of oxide components in silicate liquids. Contrib. Mineral. Petrol., 71: 117–124.

Nisbet, E.G. and Walker, D., 1982. Komatiites and the structure of the Archean mantle. Earth Planet. Sci. Lett., 60: 105–113.

Nixon, P.H. and Boyd, F.R., 1973. Petrogenesis of the granular and sheared ultrabasic nodule suite in kimberlites. In: P.H. Nixon (Editor), Lesotho Kimberlites. Lesotho National Development Corporation, Maseru, Lesotho, pp. 48–56.

O'Hara, M.J., 1968. The bearing of phase equilibria studies in synthetic and natural systems on the origin and evolution of basic and ultrabasic rocks. Earth Sci. Rev., 4: 69–113.

Ohtani, E. and Kumazawa, M., 1981. Melting of forsterite (Mg_2SiO_4) up to 15 GPa. Phys. Earth Planet. Inter., 27: 32–38.

Ohtani, E., Irifune, T. and Fujino, K., 1981. Fusion of pyrope at high pressures and rapid growth from the pyrope melt. Nature, 294: 62–64.

Presnall, D.C., Dixon, S.A., Dixon, J.R., O'Donnell, T.H., Brenner, N.L., Schrock, R.L. and Dyrus, D.W., 1978. Liquidus phase relations on the join diopside–forsterite–anorthite from 1 atm. to 20 kbar: their bearing on the generation and crystallization of basaltic magma. Contrib.

Mineral. Petrol., 66: 203–220.

Presnall, D.C., Dixon, J.R., O'Donnell, T.H. and Dixon, S.A., 1979. Generation of mid-ocean ridge tholeiites. J. Petrol., 20: 3–35.

Richter, F.M. and McKenzie, D.P., 1981. On some consequences and possible causes of layered mantle convection. J. Geophys. Res., 86: 6133–6142.

Stacey, F., 1977. A thermal model of the Earth. Phys. Earth Planet. Inter., 15: 341–348.

Stevenson, D.J., 1980. Applications of liquid state physics to the Earth's core. Phys. Earth Planet. Inter., 22: 42–52.

Stolper, E., Walker, D., Hagar, B.H. and Hays, J.F., 1981. Melt segregation from partially molten source regions: the importance of melt density and source region size. J. Geophys. Res., 86: 6261–6271.

Tuttle, O.F. and Bowen, N.L., 1958. Origin of granite in the light of experimental studies in the system $NaAlSi_3O_8$–$KAlSi_3O_8$–SiO_2–H_2O. Geol. Soc. Am., Memo., 74.

Watt, J.P. and Ahrens, T.J., 1982. The role of iron partitioning in mantle composition, evolution, and scale of convection. J. Geophys. Res., 87: 5631–5644.

Williams, D.W. and Kennedy, G.C., 1969. Melting curve of diopside to 50 kilobars. J. Geophys. Res., 74: 4359–4366.